A multilayered piezoelectric shell theory

Claire Ossadzow-David, Maurice Touratier

A multilayered piezoelectric shell theory

Claire Ossadzow-David [a,*], Maurice Touratier [b]

[a] LMM – UMR CNRS 7607, Université Paris VI, Boîte courrier No 0162, 4, Place Jussieu, 75252 Paris Cedex 05, France
[b] LMSP– UMR CNRS 8106 – ENSAM – ESEM 151, Bd de l'Hôpital, 75013 Paris Cedex, France

This paper presents a two-dimensional theory for the analysis of piezoelectric shells. The theory is based on an hybrid approach in which the continuity conditions for both mechanical and electric unknowns at layer interfaces as well as the imposed conditions on the bounding surfaces and at the interfaces are independently satisfied. Then, the piezoelectric boundary-value problem is stated using such kind of mechanical displacements and electrostatic potential, in conjunction with the coupled piezoelectric constitutive law. The accuracy of the proposed theory is assessed through investigation of significant problems, for which an exact three-dimensional solution is known.

Keywords: A. Layered structures; Piezoelectric; C. Shell theory; Continuity; Constraints

1. Introduction

The development of the so-called ''smart-structures'', e.g., made of piezoelectric composites, require nowadays more and more precision in their design and sizing. The importance of efficient models has, so far, led to numerous theories.

The modeling of piezoelectric shells mostly concerns cases attached to specific geometries (cylindrical and spherical): Toupin [1] studied the static response of a radially polarized spherical piezoelectric shell; Adelman and Stavsky [2,3] examined cases involving hollow piezoelectric cylinders. Sun and Chen [4] and Karlash [5] studied wave propagation in layered piezoelectric cylinders; Paul et al. [6,7] examined free vibration problems. Siao et al. [8] proposed a semi-analytic model for layered piezoelectric cylinders taking into account a layerwise behavior of the composite.

Analytic solutions for laminated piezoelectric cylinders were proposed by Mitchell et al. [9], Xu and Noor [10], Heyliger [11] and Dumir et al. [12].

Drumheller and Kalnins [13] used classical shell theory for free vibrations of shells of revolution. Haskins and Kalnins [14] proposed the development of electrical and mechanical quantities as expansions of the thickness variable. Tzou and Garde [15] used the Kirchhoff–Love hypothesis to derive the governing equations for thin shells, but did not take into account the charge equation. It was done by Tzou and Zhong [16], this time with a shear-deformation theory. Other piezoelectric shell models and finite element approximations, based on single-layer models, were also developed by Tzou [17]. A Reissner–Mindlin shear-deformation shell finite element with surface bonded piezoelectric layers was developed by Lammering [18]. Koconis et al. [19] used a Ritz method for three-layered shells with embedded piezoelectric actuators.

Tzou and Yee [20] proposed a coupled theory where the piezoelectric shells are considered as a layerwise assembly of curvilinear solid piezoelectric triangular elements. Heyliger et al. [21] developed a finite-element for laminated piezoelectric shells. Saravanos [22] used a coupled mixed theory for curvilinear composite piezoelectric laminates with the first-order shear deformation theory hypothesis and a layerwise approximation of the electrostatic potential, along with the corresponding finite element for piezoelectric shells.

We propose here a new two-dimensional theory for the modeling of deep multilayered piezoelectric shells. It

* Corresponding author. Fax: +33-1-44-27-52-59.
E-mail address: david@lmm.jussieu.fr (C. Ossadzow-David).

Nomenclature

V	space occupied by the shell
h	total thickness of the shell
R	radius of curvature of the shell
S_h	top surface of the shell
S_0	bottom surface of the shell
S_i	interface between the ith and $(i+1)$th layer
A	lateral surface of the shell
(x_1, x_2, z)	Cartesian coordinate system of the shell
z_i	distance between S_0 and S_i
$z_{i_{(0)}}$	distance between S_0 and the midsurface of the ith layer
$C_{kl}^{(i)}$	components of the elastic stiffness tensor of the ith layer
s_k	shear-strains
$'$	derivation with respect to the thickness coordinate z
φ	electrostatic potential
$\varphi^{1\mathrm{B}}(x_\alpha, t)$	electrostatic potential on S_0
$\varphi^{N+1,\mathrm{B}}(x_\alpha, t)$	electrostatic potential on S_h
$\varphi^{i\mathrm{B}}(x_\alpha, t)$	electrostatic potential on S_i
$\varphi^{i\mathrm{T}}(x_\alpha, t)$	electrostatic potential on S_{i+1}
$\varphi^{i\mathrm{M}}(x_\alpha, t)$	electrostatic potential on the midsurface of the ith layer
E_l	components of the electric field
D_k	components of the electric displacement
$e_{kl}^{(i)}$	components of the rotated piezoelectric tensor of the ith layer
$\varepsilon_{kl}^{(i)}$	components of the dielectric tensor of the ith layer
ρ	mass density
δ	variational operator
$\cdot$	differentiation with respect to time t
ε_0	permittivity of vacuum ($\varepsilon_0 = 8.85 \times 10^{-12}$ F/m)

extends our previous works on plates and shells [23,24] to piezoelectricity by combining our previous equivalent single-layer approach for the displacement field, with quadratic variations of the electrostatic potential through the piezoelectric layers. Both quantities are automatically continued at layer interfaces. In addition, transverse shear stresses as well as the electric displacement are independently continued, using at the first stage uncoupled constitutive law for those two fields. Refinements of the shear and membrane terms are taken into account, in the displacement field, by means of trigonometric functions. Moreover, we allow values for the electrostatic potential to be imposed either on the top and bottom surfaces of the structure, or at layer interfaces.

Finally, the piezoelectric boundary-value problem is constructed using the consistent coupled constitutive law, in conjunction with the above displacements and electrostatic potential fields. The proposed piezoelectric shell model is evaluated for significant problems, for which the exact three-dimensional solution is known [12].

2. The piezoelectric shell model

2.1. Geometric considerations for shells

We consider an undeformed laminated shell of constant thickness h, consisting of an arrangement of a finite number N of piezoelectric layers (see Fig. 1). The space occupied by the shell will be denoted V. The boundary of the shell is the reunion of the upper surface S_h, the lower surface S_0, and the edge faces A.

The interface between the ith and $(i+1)$th layer is denoted by S_i, the distance between S_0 and S_{i+1}, z_i.

The reference surface coincides with the bottom surface of the shell S_0.

In this paper, the Einsteinian summation convention applies to repeated indices, where Latin indices range from 1 to 3 while Greek indices range from 1 to 2.

The Cartesian coordinate system of the shell will be denoted by (x_1, x_2, z).

A point M out of the reference surface being given, let us denote P the point of the reference surface closest to M. Covariant base vectors $(\vec{a}_i)$, $(\vec{g}_i)$ and contravariant base vectors $(\vec{a}^i)$, $(\vec{g}^i)$ in the undeformed state of the shell are introduced such as:

$$\begin{aligned}
&\vec{a}_\alpha = \vec{P}_{,\alpha}, \quad \vec{a}_3 = \frac{\vec{a}_1 \wedge \vec{a}_2}{\left\|\vec{a}_1 \wedge \vec{a}_2\right\|}, \quad \left(\vec{a}_1 \wedge \vec{a}_2\right) \cdot \vec{a}_3 > 0, \\
&\vec{g}_i = \vec{M}_{,i}, \quad \left(\vec{g}_1 \wedge \vec{g}_2\right) \cdot \vec{g}_3 > 0, \quad \vec{a}^\alpha \cdot \vec{a}_\beta = \delta_\beta^\alpha, \\
&\vec{a}^3 = \vec{a}_3, \quad \vec{g}^\alpha \cdot \vec{g}_\beta = g_\beta^\alpha, \quad \vec{g}^3 = \vec{g}_3.
\end{aligned} \tag{1}$$

Differentiation with respect to x_i is denoted by "$_{,i}$", $[\delta_\alpha^\beta]$ being the identity tensor.

It is recalled that

$$\vec{M} = \overrightarrow{P} + z\vec{a}_3. \tag{2}$$

The above equations ensure the following relations (see, for instance [25]):

$$\begin{aligned}
&\vec{g}_\alpha = \mu_\alpha^\beta \vec{a}_\beta, \quad \vec{g}_3 = \vec{a}_3, \quad \vec{g}^\alpha = -\mu_\beta^{\alpha-1}\vec{a}^\beta, \quad \vec{g}^3 = \vec{a}^3, \\
&\vec{g}_\alpha = g_{\alpha\beta}\vec{g}^\beta, \quad \vec{g}^\alpha = g^{\alpha\beta}\vec{g}_\beta, \quad \vec{a}_\alpha = a_{\alpha\beta}\vec{a}^\beta, \quad \vec{a}^\alpha = a^{\alpha\beta}\vec{a}_\beta.
\end{aligned} \tag{3}$$

The components of the shifter tensor are denoted by

$$\mu_\beta^\alpha = \delta_\beta^\alpha - zb_\beta^\alpha, \tag{4}$$

those of the curvature tensor by

$$b_{\alpha\beta} = \vec{a}_{\alpha,\beta} \cdot \vec{a}^3, \tag{5}$$

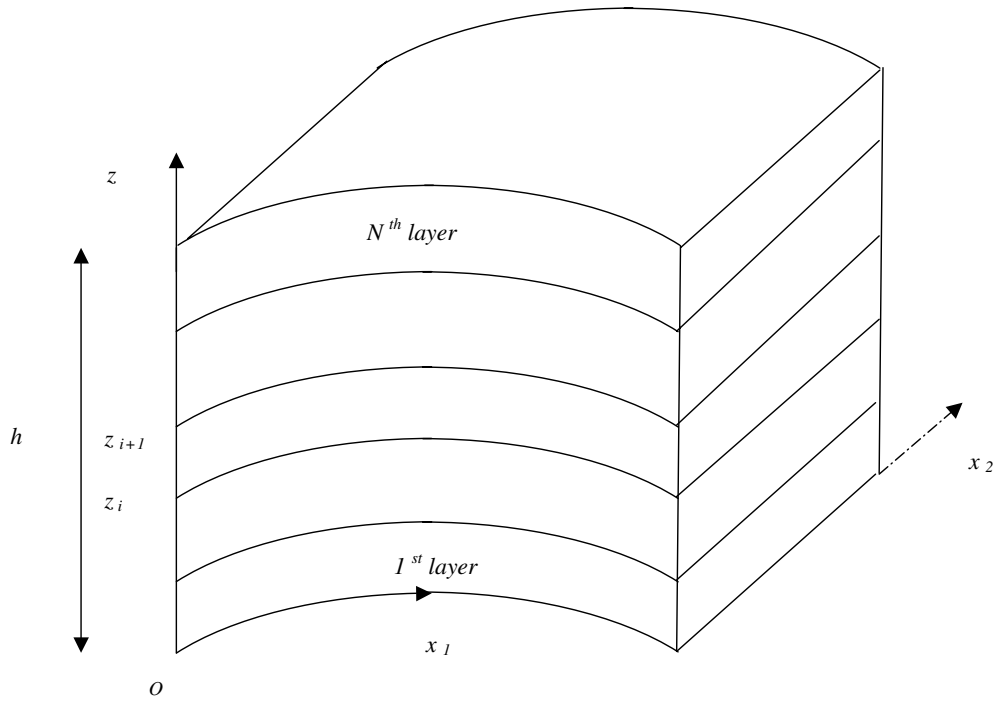

Fig. 1. The multilayered piezoelectric shell.

and its mixed components by

$$b^{\alpha}_{\beta} = -\vec{a}_{3,\beta} \cdot \vec{a}^{\alpha}. \tag{6}$$

The surface metrics α_1 and α_2 are related to the $a_{\alpha\beta}$ coefficients via

$$(a_{\alpha})^2 = a_{\alpha\alpha} \tag{7}$$

(no summation on α index).

In the following, the curvilinear coordinates (*or shell coordinates*) are assumed orthogonal, and are such that the x_1- and x_2-curves are lines of curvature on the reference surface $z = 0$; z-curves are straight lines perpendicular to the surface $z = 0$. R_1 and R_2 are the values of the principal radii of curvature of the reference surface.

The distance $\mathrm{d}s$ between two points $P(x_1, x_2, 0)$, $P'(x_1 + \mathrm{d}x_1, x_2 + \mathrm{d}x_2, 0)$ of the reference surface S_0 of the shell is given by

$$(\mathrm{d}s)^2 = \alpha_1^2(\mathrm{d}x_1)^2 + \alpha_2^2(\mathrm{d}x_2)^2, \tag{8}$$

where α_1 and α_2 are the surface metrics

$$\alpha_l^2 = \left(\frac{\partial P}{\partial x_l}\right)\left(\frac{\partial P}{\partial x_l}\right). \tag{9}$$

The distance $\mathrm{d}S$ between two points $M(x_1, x_2, z)$, $M'(x_1 + \mathrm{d}x_1, x_2 + \mathrm{d}x_2, z + \mathrm{d}z)$ out of the reference surface is given by

$$(\mathrm{d}S)^2 = L_1^2(\mathrm{d}x_1)^2 + L_2^2(\mathrm{d}x_2)^2 + L_3^2(\mathrm{d}z)^2, \tag{10}$$

where L_1, L_2 and L_3 are the so-called Lamé coefficients:

$$L_1 = \alpha_1\left(1 + \frac{z}{R_1}\right), \quad L_2 = \alpha_2\left(1 + \frac{z}{R_2}\right), \quad L_3 = 1. \tag{11}$$

2.2. Kinematic assumptions

Geometric linear shells are considered, including an elastic-linear behaviour for laminates. The transverse normal stress is ignored and it is assumed that no tangential tractions are exerted on the upper and lower surfaces of the shell.

The components of the displacement field of any point $M(x_1, x_2, z)$ of the volume occupied by the shell (V), expressed for sake of commodity in the contravariant basis $(\vec{g}^{\alpha}, \vec{g}^{3})$, are assumed in the following form:

$$\begin{cases} U_{\alpha} = u_{\alpha} + z\eta_{\alpha} + f(z)\psi_{\alpha} + g(z)\gamma^0_{\alpha} \\ \qquad +\sum_{m=1}^{N-1} u_{(m)_{\alpha}}(z - z_m)H(z - z_m), \\ U_3 = w, \end{cases} \tag{12}$$

where (as suggested in [26] for $f(z)$):

$$f(z) = \frac{h}{\pi}\sin\left(\frac{\pi z}{h}\right), \quad g(z) = \frac{h}{\pi}\cos\left(\frac{\pi z}{h}\right), \tag{13}$$

H being the *Heaviside step function*, defined by:

$$H(z - z_m) = \begin{cases} 1 & \text{for } z \geqslant z_m, \\ 0 & \text{for } z < z_m. \end{cases} \tag{14}$$

This step function has been previously used among others in Di Sciuva [27] and He [28].

Also, as in Touratier [26], the choice for $f(z)$ can be justified in a discrete-layer approach from the three-dimensional works of Cheng [29] for thick plates.

In this displacement field, u_{α} are membrane displacements, γ^0_{α} are the components of the transverse shear strain vector at $z = 0$, w is the transverse deflection of the shell.

The η_α and ψ_α are functions to be determined using the boundary conditions for the transverse shear stresses on the top and bottom surfaces of the shell. With the help of the $u_{(m)_\alpha}$, which represent the generalized "*displacements per layer*" the continuity of the displacements at layer interfaces are automatically satisfied from the Heaviside function. The generalized displacements per layer are then determined from the continuity conditions on the transverse shear stresses at the interfaces. The transverse shear-stresses in each layer are given by the classic uncoupled constitutive law

$$\sigma_{6-\alpha}^{(i)^{\text{uncoupled}}} = C_{6-\alpha,6-\alpha}^{(i)} s_{6-\alpha}, \quad i = 1, \ldots, N-1, \ \ \alpha = 1, 2, \tag{15}$$

where the $C_{6-\alpha}^{(i)}$ are the corresponding stiffness component, and $s_{6-\alpha}$ the shear strains.

The boundary conditions allow one to eliminate the η_α and ψ_α, from the following system:

$$\begin{aligned} &\eta_\alpha = -\psi_\alpha - w_{|\alpha} - b_\alpha^\nu \left[u_\nu + \frac{h}{\pi} \gamma_\nu^0 \right], \\ &-2\psi_\alpha + h b_\alpha^\nu \psi_\nu - 2\frac{h}{\pi} b_\alpha^\nu \gamma_\nu^0 + \sum_{m=1}^{N-1} \left(\delta_\alpha^\nu - b_\alpha^\nu z_m \right) u_{(m)_\nu} = 0 \end{aligned} \tag{16}$$

or

$$\psi_\alpha = d_\alpha^\beta \gamma_\beta^0 + \sum_{m=1}^{N-1} f_{(m)_\alpha}^\beta u_{(m)_\beta}, \tag{17}$$

where

$$\begin{aligned} &[d_\alpha^\beta] = [h b_\alpha^\beta - 2\delta_\alpha^\beta]^{-1} \left[2\frac{h}{\pi} b_\alpha^\beta \right], \\ &\left[f_{(m)_\alpha}^\beta \right] = \left[h b_\alpha^\beta - 2\delta_\alpha^\beta \right]^{-1} \left[\delta_\alpha^\nu - b_\alpha^\nu z_m \right], \end{aligned} \tag{18}$$

$[d_\alpha^\beta]$ being the tensor of components d_α^β, given by the first relation of the above equation.

The transverse shear stresses can then be expressed as functions of $u_{(m)_\alpha}$, γ_α^0.

The continuity conditions for transverse shear stresses lead thus to a system of $2(N-1)$ equations with the $2(N-1)$ unknowns $u_{(m)_\alpha}$.

Those latter functions can then be expressed in terms of the γ_α^0,

$$u_{(m)_\alpha} = \lambda_{(m)_\alpha} \gamma_\alpha^0 \qquad \text{(no summation on } \alpha), \tag{19}$$

where the $\lambda_{(m)_\alpha}$ are given by the resolution of the previous system.

The final form of the displacement field is given by:

$$\begin{cases} U_\alpha = \mu_\alpha^\beta u_\beta - z w_{|\alpha} + h_\alpha^\beta \gamma_\beta^0, \\ U_3 = w, \end{cases} \tag{20}$$

where h_α^β are functions of the global thickness coordinate z,

$$\begin{aligned} h_\alpha^\beta(z) = {} & g(z)\delta_\alpha^\beta - z\frac{h}{\pi} b_\alpha^\beta + [f(z) - z] d_\alpha^\beta \\ & + \sum_{m=1}^{N} \left[f_{(m)_\alpha}^\beta + (z - z_m) H(z - z_m) \delta_\alpha^\beta \right] \lambda_{(m)_\beta}. \end{aligned} \tag{21}$$

All those formulae will be referred to as *Kinematic Field* (K.F.).

This kinematic field has been developed in Ossadzow et al. [23,24].

2.3. The electrostatic potential

Within a standard variational procedure when formulating any piezoelectric boundary-value problem, it is easy to show that the piezoelectric constitutive law given by Eq. (35) introduces a strong coupling, including besides derivatives. This does not allow to exactly solve all the interfaces and boundary equations that could be used to reduce the number of unknowns (see an example in elasticity for thick plates in [30]).

Therefore, to approximate the electrostatic potential, we consider the purely electric state of the shell, as above in elasticity, in order to write interface conditions and boundary conditions at the top and bottom surfaces of the shell. Then, when formulating the piezoelectric boundary-value problem, we will include coupled electromechanical constitutive laws. Eventually, throughout several examples, we will show that using the uncoupled law just when building the displacement and electrostatic fields has not any significative influence on the distributions of stresses and electrostatic potential.

So, the electrostatic potential φ is approximated under the following form:

$$\varphi(x_1, x_2, z, t) = \sum_{i=1}^{N} \varphi^i(x_1, x_2, z, t) \chi^i(z), \tag{22}$$

where the φ^i are the potentials "per layer", and χ^i the characteristic ith-*layer function*,

$$\chi^i(z) = \begin{cases} 1 & \text{if } z \in [z^i, z^{i+1}], \\ 0 & \text{if } z \notin [z^i, z^{i+1}]. \end{cases} \tag{23}$$

Introducing, for each layer, the thickness coordinate ξ^i (see Fig. 2), given by

$$-1 \leqslant \xi^i \leqslant 1, \quad \xi^i = \frac{2(z - z_{i_{(0)}})}{h_i}, \tag{24}$$

where $z_{i_{(0)}}$ is the distance between S_0 and the midsurface of the ith layer, the φ^i are taken as

$$\begin{aligned} \varphi^i(x_j, t) = {} & \tfrac{1}{2}\xi^i(\xi^i - 1)\varphi^{i\mathrm{B}}(x_\alpha, t) + (1 - (\xi^i)^2)\varphi^{i\mathrm{M}}(x_\alpha, t) \\ & + \tfrac{1}{2}\xi^i(\xi^i + 1)\varphi^{i\mathrm{T}}(x_\alpha, t) \qquad (i = 1, \ldots, N), \end{aligned} \tag{25}$$

$\varphi^{i\mathrm{B}}(x_\alpha, t)$ is the electrostatic potential on the bottom surface S_i, $\varphi^{i\mathrm{T}}(x_\alpha, t)$ the electrostatic potential on the top surface S_{i+1}, and $\varphi^{i\mathrm{M}}(x_\alpha, t)$ the electrostatic potential on the midsurface of the ith layer (see Fig. 2), so that

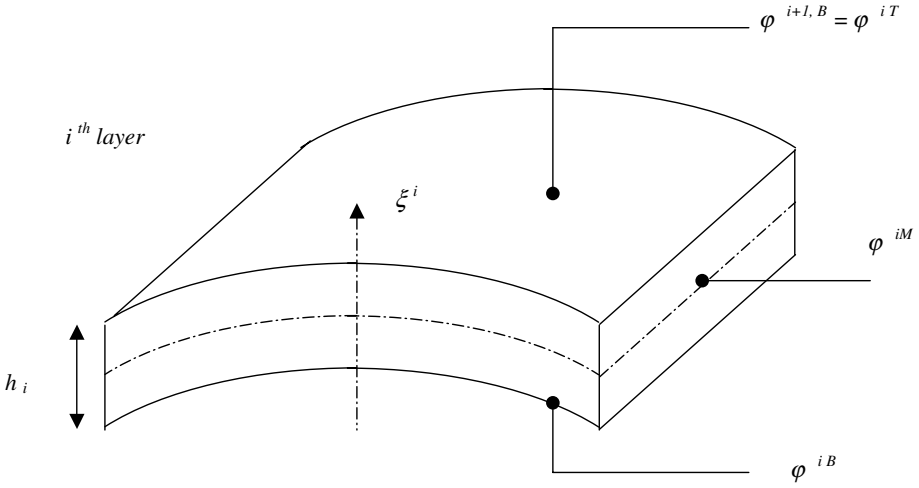

Fig. 2. Configuration of the ith layer.

$$\begin{aligned}
&\varphi^i(x_\alpha, z_i, t) = \varphi^{i\mathrm{B}}(x_\alpha, t),\\
&\varphi^i(x_\alpha, z_{i+1}, t) = \varphi^{i\mathrm{T}}(x_\alpha, t),\\
&\varphi^i\left(x_\alpha, \frac{z_{i+1}-z_i}{2}, t\right) = \varphi^{i\mathrm{M}}(x_\alpha, t) \qquad (i = 1, \ldots, N).
\end{aligned} \tag{26}$$

Since

$$\varphi^{i+1,\mathrm{B}}(x_\alpha, z_i, t) = \varphi^{i\mathrm{T}}(x_\alpha, z_i, t) \qquad (i = 0, \ldots, N) \tag{27}$$

it is worth noting that the continuity of the electrostatic potential at layer interfaces is automatically satisfied, as it can be seen in Fig. 2.

Starting from the first layer, we choose to keep $\varphi^{i\mathrm{B}}(x_\alpha, t)$ and $\varphi^{i\mathrm{M}}(x_\alpha, t)$ as unknowns.

The φ^i can then be written as

$$\begin{aligned}
\varphi^i(x_j, t) = {}& \tfrac{1}{2}\xi^i(\xi^i - 1)\varphi^{i\mathrm{B}}(x_\alpha, t) + (1 - (\xi^i)^2)\varphi^{i\mathrm{M}}(x_\alpha, t)\\
&+ \tfrac{1}{2}\xi^i(\xi^i + 1)\varphi^{i+1,\mathrm{B}}(x_\alpha, t) \quad (i = 1, \ldots, N),
\end{aligned} \tag{28}$$

where $\varphi^{1\mathrm{B}}(x_\alpha, t)$ is the electrostatic potential on S_0, $\varphi^{N+1,\mathrm{B}}(x_\alpha, t)$ the electrostatic potential on S_h (see Fig. 2).

For future applications, we suppose that p values for the electrostatic potential are given, which means that p values for the $\varphi^{i\mathrm{B}}(x_\alpha, t)$, are imposed, depending on the kind of electric boundary conditions. These values can be given on the top and bottom surfaces of the plate, or at layer interfaces.

The uncoupled piezoelectric constitutive law gives

$$D_3^{\text{uncoupled}} = \varepsilon_{33}E_3 = -\varepsilon_{33}\varphi_{,3}. \tag{29}$$

The continuity of the purely electric D_3 at layer interfaces and the boundary conditions on top and bottom surfaces and at the p layer interfaces lead to a system of $N + p - 1$ equations which allow to eliminate part of the $\varphi^{i\mathrm{B}}$ and $\varphi^{j\mathrm{M}}$, as it can be seen in the examples developed in Parts II and III.

The $\varphi^{i\mathrm{B}}$ which are chosen to remain unknown will be denoted $\{\varphi^{i_1\mathrm{B}}, \ldots, \varphi^{i_n\mathrm{B}}\}$.

The $\varphi^{j\mathrm{M}}$ which are chosen to remain unknown will be denoted $\{\varphi^{j_1\mathrm{M}}, \ldots, \varphi^{j_m\mathrm{M}}\}$.

It can be noted that

$$i_n + j_m = 2N + 1 - (N - 1 + p) = N - p + 2. \tag{30}$$

The electrostatic potential can then be written under the following form:

$$\varphi = \sum_{i=i_1}^{i_n} Q^{i\mathrm{B}}\varphi^{i\mathrm{B}} + \sum_{j=j_1}^{j_m} Q^{j\mathrm{M}}\varphi^{j\mathrm{M}}, \tag{31}$$

where the $Q^{i\mathrm{B}}$ and $Q^{j\mathrm{M}}$ are polynomial functions of the global thickness coordinate z (see examples Part II), coming from the imposed boundary conditions for the potential, as described before.

After solving as explained hereafter in Section 2.5 any boundary-value problem, both all the mechanical unknowns, and the unknowns electrostatic potential are the obtained. The only electric quantity that cannot be obtained without a post-processing correction is the final (coupled) electric displacement: we recall that the coupled piezoelectric constitutive law gives

$$D_3^{\text{coupled}} = \varepsilon_{33}E_3 + e_{3j}s_j. \tag{32}$$

It is very important to note that the $\varepsilon_{33}E_3$ term are very small compared to the $e_{3j}s_j$ terms; hence, if the final value of the electric displacement is not corrected in a post-processing phase, the $e_{3j}s_j$ terms will prevail on the $\varepsilon_{33}E_3$ term. The $e_{3j}s_j$ terms are not continued at layer interfaces (see (29)). Thus, the final electric displacement requires such a correction. This correction leads to the following corrected value, which satisfies continuity at layer interfaces

$$\begin{aligned}
\tilde{D}_3^{\text{coupled}} = {}& \varepsilon_{33}E_3 + e_{3j}s_j\\
&- \left[e_{3j}^{(k)}s_j^{(k)}(z_k)\chi^k(z) - e_{3j}^{(k+1)}s_j^{(k+1)}(z_k)\chi^{k+1}(z)\right],
\end{aligned} \tag{33}$$

where the (k) exponent characterizes the quantities related to the kth layer and the $(k+1)$ exponent the quantities related to the $(k+1)$th layer.

For sake of commodity, we will denote by $\tilde{D}^{\text{coupled}}$ the final (coupled) electric displacement field (only its third component being of course corrected).

Therefore, at the kth layer interface, the continuity of the modified coupled electric displacement $\tilde{D}_3^{\text{coupled}}$ is satisfied ($\varepsilon_{33}E_3$) being continuous, from Eqs. (17)–(20), since we have:

$$\begin{aligned}\lim_{\substack{z\to z_{k'}\\ z<z_k}} \tilde{D}_3^{\text{coupled}} &= \lim_{\substack{z\to z_{k'}\\ z<z_k}} \left\{ \varepsilon_{33}E_3 + \underbrace{e_{3j}s_j - e_{3j}^{(k)}s_j^{(k)}(z_k)}_{0} \right\} \\ &= \lim_{z\to z_k}\{\varepsilon_{33}E_3\} \\ &= \lim_{\substack{z\to z_{k'}\\ z>z_k}} \left\{ \varepsilon_{33}E_3 + \underbrace{e_{3j}s_j - e_{3j}^{(k+1)}s_j^{(k+1)}(z_k)}_{0} \right\}.\end{aligned} \tag{34}$$

Hereafter, depending on the kind of electric boundary conditions, we will show how to build the potential field, since our method is new as it is possible to check, and different from a usual layerwise method, which does not exploit all the boundary conditions. It allows to reduce the size of any boundary-value problem.

2.4. The linear-piezoelectric constitutive law

The constitutive law of a piezoelectric material, adopted in our model, has been given by Tiersten [31], and is expressed by:

$$\begin{cases} \sigma_i^{\text{coupled}} = C_{ij}s_j - e_{ki}E_k, \\ D_k^{\text{coupled}} = \varepsilon_{kl}E_l + e_{ki}s_i, \end{cases} \tag{35}$$

where σ_i are the components of the stress tensor, C_{ij} the elastic stiffness components, s_j the components of small strain, e_{ki} the piezoelectric coefficients, E_l the components of the electric field, D_k the components of the electric displacement, and ε_{kl} are the dielectric constants. The standard contracted notation, with $i,j = 1,\ldots,6$ and $k,l = 1,\ldots,3$, has been used in these equations. The poling direction is coincident with the z-axis.

Using results stated in Section 2.3, the electric-field is related to the electrostatic potential φ through the relation

$$\vec{E} = -\vec{\text{grad}}\varphi = -\sum_{i=i_1}^{i_n} \vec{\text{grad}}\left[Q^{i\text{B}}\varphi^{i\text{B}}\right] - \sum_{j=j_1}^{j_m} \vec{\text{grad}}\left[Q^{j\text{M}}\varphi^{j\text{M}}\right]. \tag{36}$$

For the materials used in this study, we assume that the nonzero components of the rotated piezoelectric tensor e_{ki}, the elastic stiffness tensor C_{ij}, and the components of the dielectric tensor ε_{kl} are those of orthorhombic crystal. The nonzero elements of those two latter tensors will be taken as e_{31}, e_{32}, e_{33}, e_{24}, e_{15} and ε_{11}, ε_{22}, ε_{33}.

Taking, as usually for plates, into account a zero value of the transverse normal stress, the constitutive law "*per layer*" can be written as follows:

$$\sigma_i^{\text{coupled}} = C_{ij}^{2D}s_j - e_{ki}^{2D}E_k, \quad D_k^{\text{coupled}} = \varepsilon_{kl}^{2D}E_l + e_{kj}^{2D}s_j, \tag{37}$$

where

$$\begin{aligned} C_{ij}^{2D} &= C_{ij} - C_{i3}\frac{C_{3j}}{C_{33}}, \quad e_{ki}^{2D} = e_{ki} - C_{i3}\frac{e_{k3}}{C_{33}}, \\ \varepsilon_{kl}^{2D} &= \varepsilon_{kl} + e_{k3}\frac{e_{l3}}{C_{33}}. \end{aligned} \tag{38}$$

2.5. The two-dimensional boundary-value problem

The equations of motion and the natural boundary conditions are derived via Hamilton's principle:

$$\begin{aligned}\int_0^t \Bigg\{ &\int_V \sigma^i\delta s_i \,\mathrm{d}V + \int_V D_i\delta\varphi_{,i}\,\mathrm{d}V + \int_V \vec{f}_v\cdot\delta\vec{U}\,\mathrm{d}V \\ &+ \int_A \vec{f}_s\cdot\delta\vec{U}\,\mathrm{d}A + \int_{S_0}(-p_h\mu_h + p_0)\,\mathrm{d}S + \int_S W\delta\varphi\,\mathrm{d}V \Bigg\}\mathrm{d}t \\ &= 0.\end{aligned} \tag{39}$$

A superposed dot is used for differentiation with respect to time t; ρ is the mass density, and δ the variational operator; f_v^i are components of body forces; f_s^i the prescribed components of the load on the undeformed lateral surface of the shell, p_0 and p_h the prescribed components of traction on the surfaces S_0 and S_h. W is the density of electric forces. μ_h is the value of the determinant of the shifter tensor at $z = h$.

Performing numerical integration through the thickness of the shell, the following equations of motion are deduced from Eq. (39), (K.F.), and (31):

$$\begin{aligned} &N_{(1)_{|\lambda}}^{\alpha\lambda} + N_{(2)_{|\beta}}^{\alpha\beta} = I_1\ddot{u}_\alpha - I_2\ddot{w}_{|\alpha} + I_3^\alpha\ddot{\gamma}_\alpha^0, \\ &N_{(3)} + M_{(1)_{|\alpha\nu}}^{\alpha\nu} + M_{(2)_{|\beta\nu}}^{\beta\nu} = I_2\ddot{u}_{\alpha|\alpha} - I_4\ddot{w}_{|\alpha\alpha} + I_5^\alpha\ddot{\gamma}_{\alpha|\alpha}^0 + I_1\ddot{w}, \\ &\left[N_{(5)_{|\lambda}}^{\alpha\lambda} + N_{(6)_{|\beta}}^{\alpha\beta} + N_{(4)}^{\alpha}\right] = I_3^\alpha\ddot{u}_\alpha - I_5^\alpha\ddot{w}_{|\alpha} + I_6^\alpha\ddot{\gamma}_\alpha^0, \\ &\mathcal{N}^{i\text{B}} + \mathcal{M}_{|\alpha}^{i\text{B}^\alpha} = 0, \quad i\in\{i_1,\ldots,i_n\}, \\ &\mathcal{N}^{j\text{M}} + \mathcal{M}_{|\alpha}^{j\text{M}^\alpha} = 0, \quad j\in\{j_1,\ldots,j_m\} \quad (\alpha = 1,2). \end{aligned} \tag{40}$$

We introduce

$$\Delta_{\alpha\beta} = 1 - \delta_\beta^\alpha. \tag{41}$$

We will denote by μ the determinant of the shifter tensor.

In Eq. (40):

- the generalized stresses are given by:

$$N^{\alpha\lambda}_{(1)} = -\int_0^h \left\{C_{\lambda j}s_j - e_{3\alpha}E_3\right\}\mu^{\nu}_{\lambda}\mu^{\alpha}_{\nu}\mu\,\mathrm{d}z;$$

$$N^{\alpha\beta}_{(2)} = -\int_0^h C_{6,6}s_6\Delta_{\lambda\beta}\mu^{\nu}_{\lambda}\mu^{\alpha}_{\nu}\mu\,\mathrm{d}z;$$

$$N_{(3)} = -\int_0^h \left[\left\{C_{\alpha j}s_j - e_{3\alpha}E_3\right\}\mu^{\nu}_{\alpha}b_{\nu\alpha} + C_{6,6}s_6\Delta_{\alpha\beta}\mu^{\nu}_{\alpha}b_{\nu\beta}h_{\alpha}\right]\mu\,\mathrm{d}z;$$

$$N^{\alpha}_{(4)} = \int_0^h \left\{C_{6-\lambda,6-\lambda}s_{6-\lambda} - e_{k,6-\lambda}E_k\right\}[\mu^{\nu}_{\lambda}h^{\alpha}_{\nu,3}. + b^{\nu}_{\lambda}h^{\alpha}_{\nu}]\mu\,\mathrm{d}z;$$

$$N^{\alpha\lambda}_{(5)} = -\int_0^h \left\{C_{\lambda j}s_j - e_{3\alpha}E_3\right\}\mu^{\nu}_{\lambda}h^{\alpha}_{\nu}\mu\,\mathrm{d}z;$$

$$N^{\alpha\beta}_{(6)} = -\int_0^h C_{6,6}s_6\Delta_{\lambda\beta}\mu^{\nu}_{\lambda}h^{\alpha}_{\nu}\mu\,\mathrm{d}z;$$

$$M^{\alpha\nu}_{(1)} = -\int_0^h \left[\left\{C_{\alpha j}s_j - e_{3\alpha}E_3\right\}\mu^{\nu}_{\alpha} + C_{6,6}s_6\Delta_{\alpha\beta}\mu^{\nu}_{\alpha}\right]\mu z\,\mathrm{d}z;$$

$$M^{\beta\nu}_{(2)} = -\int_0^h C_{6,6}s_6\Delta_{\alpha\beta}\mu^{\nu}_{\alpha}z\mu\,\mathrm{d}z;$$

$$\mathscr{N}^{i\mathrm{B}} = \int_0^h E_3\varepsilon_{33}Q^{i\mathrm{B}'}\mu\,\mathrm{d}z, \quad i\in\{i_1,\ldots,i_n\};$$

$$\mathscr{N}^{j\mathrm{M}} = \int_0^h E_3\varepsilon_{33}Q^{j\mathrm{M}'}\mu\,\mathrm{d}z, \quad j\in\{j_1,\ldots,j_m\};$$

$$\mathscr{M}^{i\mathrm{B}^{\alpha}} = -\int_0^h \{E_{\alpha}\varepsilon_{\alpha\alpha} + e_{k\alpha}s_{\alpha,\alpha}\}Q^{i\mathrm{B}}\mu\,\mathrm{d}z, \quad i\in\{i_1,\ldots,i_n\};$$

$$\mathscr{M}^{i\mathrm{M}^{\alpha}} = -\int_0^h \{E_{\alpha}\varepsilon_{\alpha\alpha} + e_{k\alpha}s_{\alpha,\alpha}\}Q^{i\mathrm{M}}\mu\,\mathrm{d}z, \quad j\in\{j_1,\ldots,j_m\}; \tag{42}$$

- the generalized external mechanical forces by:

$$F^1_{v_{\alpha}} = \int_0^h f_{v_{\alpha}}\mu\,\mathrm{d}z; \quad F^2_{v_{\alpha}} = -\int_0^h f_{v_{\alpha}}z\mu\,\mathrm{d}z;$$

$$F^3_{v_{\alpha}} = \int_0^h f_{v_{\alpha}}h_{\alpha}\mu\,\mathrm{d}z, \qquad F^3_{v} = \int_0^h f_{v_3}\mu\,\mathrm{d}z; \quad P = -p_h + p_0; \tag{43}$$

- the generalized external electrostatic forces by:

$$W^{i\mathrm{B}} = \int_0^h WQ^{i\mathrm{B}}\mu\,\mathrm{d}z, \quad i\in\{i_1,\ldots,i_n\};$$
$$W^{j\mathrm{M}} = \int_0^h WQ^{j\mathrm{M}}\mu\,\mathrm{d}z, \quad j\in\{j_1,\ldots,j_m\}; \tag{44}$$

- and the inertia terms by:

$$I_1 = \int_0^h \rho\mu\,\mathrm{d}z, \quad I_2 = \int_0^h \rho z\mu\,\mathrm{d}z,$$
$$I^{(\alpha)}_3 = \int_0^h \rho h_{\alpha}(z)\mu\,\mathrm{d}z, \quad I_4 = \int_0^h \rho z^2\mu\,\mathrm{d}z, \tag{45}$$
$$I^{(\alpha)}_5 = \int_0^h \rho z h_{\alpha}(z)\mu\,\mathrm{d}z, \quad I^{(\alpha)}_6 = \int_0^h \rho z h^2_{\alpha}(z)\mu\,\mathrm{d}z.$$

The boundary conditions for the shell leading to a "regular problem" are:

$$\left[N^{\alpha}_{(1)}n_{\alpha} + N^{\alpha\beta}_{(2)}n_{\beta}\right] = F^1_{v_{\alpha}} \quad \text{or} \quad \delta u_{\alpha} = 0,$$
$$\left[M^{\alpha}_{(1)_{,\alpha}} + M^{\alpha\beta}_{(2)_{,\beta}}\right] = F^2_{v_{\alpha}} \quad \text{or} \quad \delta w = 0,$$
$$N^{\alpha\beta}_{(4)}n_{\beta} = F^3_{v_{\alpha}} \quad \text{or} \quad \delta\gamma^0_{\alpha} = 0,$$
$$\left[M^{\alpha}_{(1)}n_{\alpha} + M^{\alpha\beta}_{(2)}n_{\beta}\right] = F_{v_3} \quad \text{or} \quad \delta w_{,\alpha} = 0;$$
$$\mathscr{M}^{i\mathrm{B}^{\alpha}}n_{\alpha} = W^{i\mathrm{B}} \quad \text{or} \quad \delta\varphi^{i\mathrm{B}} = 0, \quad i\in\left\{i_1,\ldots,i_n\right\};$$
$$\mathscr{M}^{j\mathrm{M}^{\alpha}}n_{\alpha} = W^{j\mathrm{M}} \quad \text{or} \quad \delta\varphi^{j\mathrm{M}} = 0, \quad j\in\{j_1,\ldots,j_m\}. \tag{46}$$

The equations of motion are deduced from Eq. (40) including the constitutive law given by Eqs. (35)–(38), (K.F.), Eqs. (31) and (42).

3. Validation of the piezoelectric shell model

In order to assess the accuracy of the present theory, we have considered problems for which a three-dimensional solution exists:

- first, the free vibrations of five-layered piezoelectric plates;
- second, a cylindrical orthotropic panel under pressure.

We recall that the electric-field is related to the electrostatic potential φ through the relation

$$\vec{E} = -\overrightarrow{\mathrm{grad}}\varphi, \tag{47}$$

which gives here:

$$E_1 = -\frac{\partial\varphi}{(R+z)\partial x_1}, \quad E_2 = -\frac{\partial\varphi}{(R+z)\partial x_2}, \quad E_3 = -\frac{\partial\varphi}{\partial z}. \tag{48}$$

The piezoelectric and dielectric coefficients being very small compared to the elastic constants, we introduce non-dimensional quantities:

$$C^{2D^*}_{ij} = \frac{C^{2D}_{ij}}{C_0}, \quad e^{2D^*}_{ki} = E_0\frac{e^{2D}_{ki}}{C_0}, \quad \varepsilon^{2D^*}_{kl} = E^2_0\frac{\varepsilon^{2D}_{kl}}{C_0}, \tag{49}$$

where

$$C_0 = C^1_{11} \tag{50}$$

and

$$E_0 = 10^{10}\ \mathrm{V/m}. \tag{51}$$

Then the generalized displacements and potentials are written as follows:

$$\left(\bar{u}_{\alpha}, \bar{w}, \bar{\gamma}_{\alpha}, \bar{\varphi}^{i\mathrm{B}}, \bar{\varphi}^{j\mathrm{M}}\right) = \left(C_0u_{\alpha}, C_0w, C_0\gamma^0_{\alpha}, \frac{C_0\varphi^{i\mathrm{B}}}{E_0}, \frac{C_0\varphi^{j\mathrm{M}}}{E_0}\right). \tag{52}$$

3.1. Free vibrations of five-layered piezoelectric plates

For this example, we consider a square, simply supported five-layered piezoelectric plate, in closed circuit ($\varphi = 0$ at the top and bottom surfaces of the plates).

The simple support conditions for a square plate of length a are simulated by:

$$
\begin{aligned}
&u_1(x_1,0,z,t) = u_1(x_1,a,z,t) = 0,\\
&u_2(0,x_2,z,t) = u_2(a,x_2,z,t) = 0,\\
&w(x_1 0,z,t) = w(x_1,a,z,t) = 0,\\
&w(0,x_2,z,t) = w(a,x_2,z,t) = 0,\\
&\gamma_1^0(x_1,0,z,t) = \gamma_1^0(x_1,a,z,t) = 0,\\
&\gamma_2^0(0,x_2,z,t) = \gamma_2^0(a,x_2,z,t) = 0.
\end{aligned}
\tag{53}
$$

The height of the plate is fixed at $h = 0.01$ m.

The external layers are made of PZT4, the three internal ones being a symmetric elastic Epoxy 0/90/0 cross-ply (see Table 1 for all the piezoelectric properties of those materials, ε_0 being the permittivity of vacuum). The same unit mass density will be used for all materials.

The piezoelectric coefficients of the three internal layers are identical; as for the dielectric coefficients, the three elastic layers have the same ε_{33}. The ε_{11} and ε_{22} are very close. We therefore consider that those three layers behave, on the electric point of view, as a single layer. The five-layered plate will thus be modelled as a three-layered elastic one, its core being the elastic–epoxy cross-ply.

From Eqs. (22) and (25), the approximation of the electrostatic potential becomes thus:

$$
\begin{aligned}
\varphi(x_j,t) = &\left[\frac{1}{2}\xi^1(\xi^1-1)\varphi^{1\mathrm{B}}(x_\alpha,t) + (1-(\xi^1)^2)\varphi^{1\mathrm{M}}(x_\alpha,t)\right.\\
&\left.+\frac{1}{2}\xi^1(\xi^1+1)\varphi^{2\mathrm{B}}(x_\alpha,t)\right]\chi^1\\
&+\left[\frac{1}{2}\xi^2(\xi^2-1)\varphi^{2\mathrm{B}}(x_\alpha,t) + (1-(\xi^2)^2)\varphi^{2\mathrm{M}}(x_\alpha,t)\right.\\
&\left.+\frac{1}{2}\xi^2(\xi^2+1)\varphi^{3\mathrm{B}}(x_\alpha,t)\right]\chi^2\\
&+\left[\frac{1}{2}\xi^3(\xi^3-1)\varphi^{3\mathrm{B}}(x_\alpha,t) + (1-(\xi^3)^2)\varphi^{3\mathrm{M}}(x_\alpha,t)\right.\\
&\left.+\frac{1}{2}\xi^3(\xi^3+1)\varphi^{4\mathrm{B}}(x_\alpha,t)\right]\chi^3.
\end{aligned}
\tag{54}
$$

Table 1
Elastic, piezoelectric and dielectric properties of PZT4, PVDF and Epoxy

Moduli	PZT4	PVDF	Graphite–Epoxy
C_{1111} (GPa)	139	238.24	134.86
C_{2222} (GPa)	139	23.6	14.352
C_{3333} (GPa)	115	10.64	14.352
C_{1122} (GPa)	77.8	3.98	5.1563
C_{1133} (GPa)	74.3	2.19	5.1563
C_{2233} (GPa)	74.3	1.92	7.1329
C_{2323} (GPa)	25.6	2.15	3.606
C_{1313} (GPa)	25.6	4.4	5.654
C_{1212} (GPa)	30.6	6.43	5.654
e_{31} (C/m^2)	−5.2	−0.13	0
e_{32} (C/m^2)	−5.2	−0.145	0
e_{33} (C/m^2)	15.1	−0.276	0
e_{24} (C/m^2)	12.7	−0.009	0
$\varepsilon_{11}/\varepsilon_0$	1475	12.5	3.5
$\varepsilon_{22}/\varepsilon_0$	1475	11.98	3.0
$\varepsilon_{33}/\varepsilon_0$	1300	11.98	3.0

The plate being in closed circuit,

$$
\varphi^{1\mathrm{B}}(x_\alpha,t) = \varphi^{4\mathrm{B}}(x_\alpha,t) = 0. \tag{55}
$$

Moreover, the symmetry allows to impose:

$$
\varphi^{2\mathrm{B}}(x_\alpha,t) = \varphi^{3\mathrm{B}}(x_\alpha,t), \quad \varphi^{1\mathrm{M}}(x_\alpha,t) = \varphi^{3\mathrm{M}}(x_\alpha,t). \tag{56}
$$

This results in

$$
\begin{aligned}
\varphi(x_j,t) = &\left[(1-(\xi^1)^2)\varphi^{1\mathrm{M}}(x_\alpha,t) + \frac{1}{2}\xi^1(\xi^1+1)\varphi^{2\mathrm{B}}(x_\alpha,t)\right]\chi^1\\
&+\left[\frac{1}{2}\xi^2(\xi^2-1)\varphi^{2\mathrm{B}}(x_\alpha,t) + (1-(\xi^2)^2)\varphi^{2\mathrm{M}}(x_\alpha,t)\right.\\
&\left.+\frac{1}{2}\xi^2(\xi^2+1)\varphi^{2\mathrm{B}}(x_\alpha,t)\right]\chi^2\\
&+\left[\frac{1}{2}\xi^3(\xi^3-1)\varphi^{2\mathrm{B}}(x_\alpha,t) + (1-(\xi^3)^2)\varphi^{1\mathrm{M}}(x_\alpha,t)\right]\chi^3.
\end{aligned}
\tag{57}
$$

Due to the symmetries, the continuity of the uncoupled electric displacement D_3 at layer interfaces is written at the first interface:

$$
-\varepsilon_{33}^1\varphi_{,3}^1(x_\alpha,z_1,t) = -\varepsilon_{33}^2\varphi_{,3}^2(x_\alpha,z_1,t), \tag{58}
$$

where ε_{33}^i is the dielectric coefficient corresponding to the ith layer.

This leads to an equation which allows to express $\varphi^{2\mathrm{B}}$ in terms of $\varphi^{1\mathrm{M}}$ and $\varphi^{2\mathrm{M}}$

$$
\varphi^{2\mathrm{B}}(x_\alpha,t) = \lambda^{2\mathrm{B},1\mathrm{M}}\varphi^{1\mathrm{M}}(x_\alpha,t) + \lambda^{2\mathrm{B},2\mathrm{M}}\varphi^{2\mathrm{M}}(x_\alpha,t), \tag{59}
$$

where $\lambda^{2\mathrm{B},1\mathrm{M}}$ and $\lambda^{2\mathrm{B},2\mathrm{M}}$ are the coefficients given by the resolution of the system (58).

The electrostatic potential can then be written under the following form:

$$
\varphi(x_j,t) = Q^{1\mathrm{M}}(z)\varphi^{1\mathrm{M}}(x_\alpha,t) + Q^{2\mathrm{M}}(z)\varphi^{2\mathrm{M}}(x_\alpha,t), \tag{60}
$$

where

$$
\begin{aligned}
Q^{1\mathrm{M}}(z) = &\left[(1-(\xi^1)^2) + \frac{1}{2}\xi^1(\xi^1+1)\lambda^{2\mathrm{B},1\mathrm{M}}\right]\chi^1\\
&+\left[\frac{1}{2}\xi^2(\xi^2-1)\lambda^{2\mathrm{B},1\mathrm{M}} + \frac{1}{2}\xi^2(\xi^2+1)\lambda^{2\mathrm{B},1\mathrm{M}}\right]\chi^2\\
&+\left[(1-(\xi^3)^2) + \frac{1}{2}\xi^3(\xi^3-1)\lambda^{2\mathrm{B},1\mathrm{M}}\right]\chi^3,\\
Q^{2\mathrm{M}}(z) = &\left[\frac{1}{2}\xi^1(\xi^1+1)\lambda^{2\mathrm{B},2\mathrm{M}}\right]\chi^1\\
&+\left[\frac{1}{2}\xi^2(\xi^2-1)\lambda^{2\mathrm{B},2\mathrm{M}} + (1-(\xi^2)^2)\right.\\
&\left.+\frac{1}{2}\xi^2(\xi^2+1)\lambda^{2\mathrm{B},2\mathrm{M}}\right]\chi^2 + \left[\frac{1}{2}\xi^3(\xi^3-1)\lambda^{2\mathrm{B},2\mathrm{M}}\right]\chi^3.
\end{aligned}
\tag{61}
$$

The mechanical generalized displacements remaining unknowns are u_α, w, γ_α^0. The electrical generalized unknowns are $\varphi^{1\mathrm{M}}, \varphi^{2\mathrm{M}}$.

The solution of Eqs. (40)–(46), including Eqs. (20), (37), (60), in terms of the generalized unknowns given by Eq. (52), is searched under the form:

$$\begin{cases} \bar{u}_1(x_\alpha,t) = A_1\,\mathrm{e}^{\mathrm{j}\omega t}\cos p_1x_1\sin p_2x_2, \\ \bar{u}_2(x_\alpha,t) = A_2\,\mathrm{e}^{\mathrm{j}\omega t}\sin p_1x_1\cos p_2x_2, \\ \bar{w}(x_\alpha,t) = B\,\mathrm{e}^{\mathrm{j}\omega t}\sin p_1x_1\sin p_2x_2, \\ \bar{\gamma}_1(x_\alpha,t) = C_1\,\mathrm{e}^{\mathrm{j}\omega t}\cos p_1x_1\sin p_2x_2, \\ \bar{\gamma}_2(x_\alpha,t) = C_2\,\mathrm{e}^{\mathrm{j}\omega t}\sin p_1x_1\cos p_2x_2 \end{cases} \tag{62}$$

and

$$\begin{aligned} \bar{\varphi}^{1\mathrm{M}}(x_\alpha,t) &= \Phi_1\,\mathrm{e}^{\mathrm{j}\omega t}\sin p_1x_1\sin p_2x_2, \\ \bar{\varphi}^{2\mathrm{M}}(x_\alpha,t) &= \Phi_2\,\mathrm{e}^{\mathrm{j}\omega t}\sin p_1x_1\sin p_2x_2, \end{aligned} \tag{63}$$

where

$$p_1 = p_2 = \pi/a, \tag{64}$$

which characterizes the propagation of harmonic plane-waves. The boundary conditions (the plate is simply supported) are satisfied.

Substituting these expressions into the equations of motion given by Eq. (40) with Eqs. (42)–(46) and (K. F.), (37), (60), for free motions, seven linear equations in terms of A_1, A_2, B, C_1, C_2, Φ_1 and Φ_2 are obtained. For a nontrivial solution, the determinant of the matrix of coefficients A_1, A_2, B, C_1, C_2, Φ_1 and Φ_2 must vanish, resulting in the following frequency equation:

$$\det[K^1 - \omega^2 M] = 0. \tag{65}$$

The coefficients of the corresponding stiffness matrix K^1 and mass matrix M are given in Appendix A.

The circular frequencies corresponding to the two first thickness modes are shown in Table 2.

They can be compared to those of the exact solution of Heyliger [32].

A good accuracy of our model can be noted for a thick plate ($a/h = 4$).

We conclude that since our model is in very good agreement with the exact three-dimensional solution, it is efficient, because for this five-layered piezoelectric plate it keeps only five generalized displacements and two generalized electrostatic potentials as unknowns.

3.2. Single-layered shell

For this example, we consider an infinitely long, simply supported, orthotropic, piezoelectric, radially polarized, circular cylindrical shell panel in cylindrical bending, under pressure, in closed circuit. We denote by R its mean radius, by h its thickness, and α its angular span (see Fig. 3). We will denote by θ the angular co-ordinate.

Its lateral surfaces are subjected to electrical (closed circuit) and traction (pressure on its top face) boundary conditions independent of the thickness coordinate.

The stresses, strains, displacements, electric field and potential do not depend on the x_2 variable. The displacement U_2 playing no role, it can be cancelled out.

The height of the panel is fixed at $h = 0.01$ m, and its angular span to $\alpha = \pi/3$.

The simple support conditions for the panel are simulated by:

$$\begin{aligned} &\gamma_1^0(\theta = 0) = \gamma_1^0(\theta = \alpha) = 0, \\ &w(\theta = 0) = w(\theta = \alpha) = 0. \end{aligned} \tag{66}$$

The panel is subjected to a simply sinusoidal force density on its top face,

$$p(x_1) = p_0 \sin p_1x_1, \tag{67}$$

where

$$p_1 = \pi/\alpha \tag{68}$$

and is in closed circuit. The value of p_0 is set to 10 N/m^2 The shear stresses on the top and bottom faces are specified to be zero.

The properties of the materials used in this example (PZT4) are shown in Table 1.

From Eq. (28), the approximation of the electrostatic potential becomes thus

$$\begin{aligned} \varphi(x_j) = {} & \frac{1}{2}\xi^1(\xi^1 - 1)\varphi^{1\mathrm{B}}(x_\alpha) + (1 - (\xi^1)^2)\varphi^{1\mathrm{M}}(x_\alpha) \\ & + \frac{1}{2}\xi^1(\xi^1 + 1)\varphi^{2\mathrm{B}}(x_\alpha). \end{aligned} \tag{69}$$

The shell being in closed circuit,

$$\varphi^{1\mathrm{B}}(x_\alpha) = \varphi^{2\mathrm{B}}(x_\alpha) = 0. \tag{70}$$

This results in

$$\varphi(x_j) = (1 - (\xi^1)^2)\varphi^{1\mathrm{M}}(x_\alpha) \tag{71}$$

which can be written under the following form:

$$\varphi(x_j) = Q^{1\mathrm{M}}(z)\varphi^{1\mathrm{M}}(x_\alpha) \tag{72}$$

with

$$Q^{1\mathrm{M}}(z) = (1 - (\xi^1)^2) \tag{73}$$

The mechanical generalized displacements remaining unknowns are u_1, w, γ_1^0, while the electrical generalized unknown is $\varphi^{1\mathrm{M}}$.

The solution, in terms of the generalized unknowns, is searched under the following form:

$$\begin{cases} \bar{u}_1(x_1) = A_1\cos p_1x_1, \\ \bar{w}(x_1) = B\sin p_1x_1, \\ \bar{\gamma}_1^0(x_1) = C_1\cos p_1x_1 \end{cases} \tag{74}$$

Table 2
Frequency parameters for the five-layered piezoelectric plates

	$\gamma = \omega/100$ (rad/s)	
	Model	Exact solution
$a/h = 4$	194,903	191,301
	251,763	250,769
$a/h = 50$	15592.3	15,681
	209,479	209,704

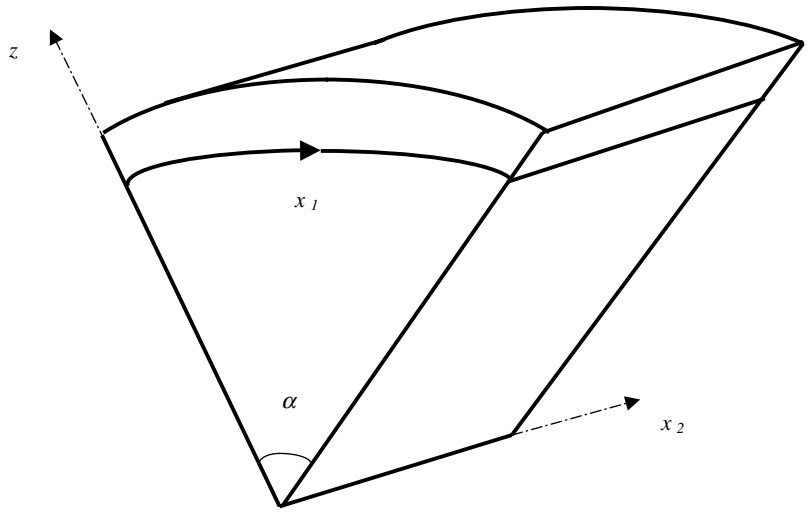

Fig. 3. The cylindrical panels.

and

$$\bar{\varphi}^{1M}(x_1) = \Phi_1 \sin p_1 x_1. \tag{75}$$

Substituting these expressions into the equilibrium equations given by Eqs. (40)–(46), with Eqs. (20), (37), (72), a linear system of the following form:

$$K^2 X^2 = B^2 \tag{76}$$

is obtained, where

$$X^2 = (A_1, B, C_1, \Phi_1). \tag{77}$$

The coefficients of K^2 and B^2 are given in Appendix B.

This system is solved using the *LinearSolve* procedure of *Mathematica* [33].

With Eqs. (20), (36) and (37), the displacement, strain and stress components, and the electrostatic potential can be calculated.

Through the thickness distribution of the normalized electrostatic potential

$$\bar{\varphi}(z) = \frac{\varphi\left(\theta = \frac{\alpha}{2}, z\right)}{\varphi\left(\theta = \frac{\alpha}{2}, \frac{h}{2}\right)}, \tag{78}$$

the normalized shear-stress

$$\bar{\sigma}_{13}(z) = \frac{\sigma_{13}(\theta = 0, z)}{\sigma_{13}\left(\theta = 0, \frac{h}{2}\right)}, \tag{79}$$

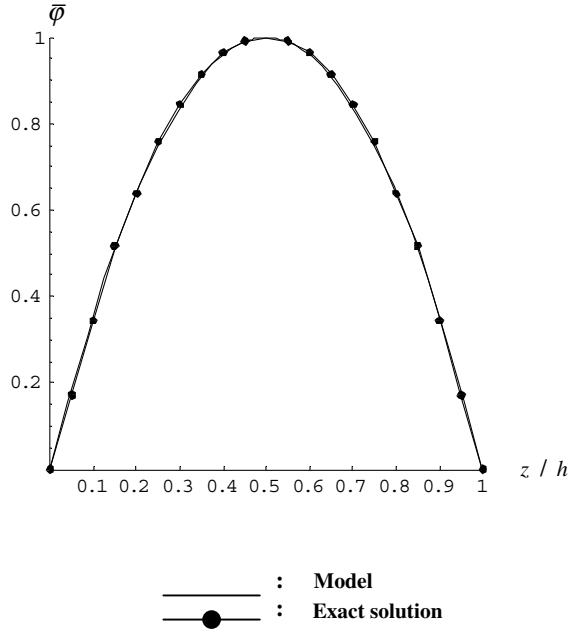

Fig. 4. Thickness distribution of the normalized electrostatic potential $\bar{\varphi}$, single-layered shell, $R = 4$ h.

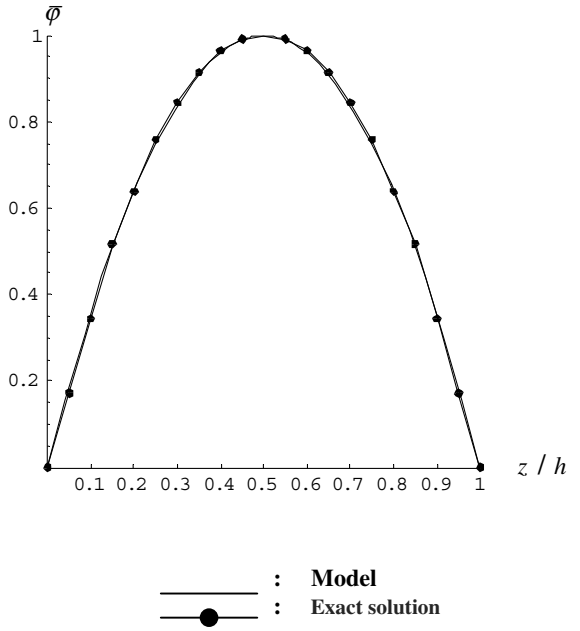

Fig. 5. Thickness distribution of the normalized electrostatic potential $\bar{\varphi}$, single-layered shell, $R = 10$ h.

and the normalized in plane stress

$$\bar{\sigma}_{11}(z) = \frac{\sigma_{11}\left(\theta = \frac{\alpha}{2}, z\right)}{\sigma_{11}\left(\theta = \frac{\alpha}{2}, 0\right)} \tag{80}$$

for different values of the ratio R/h, are shown in Figs. 4–12. The results obtained with our model are compared to the exact three-dimensional solution referred to by Dumir [12].

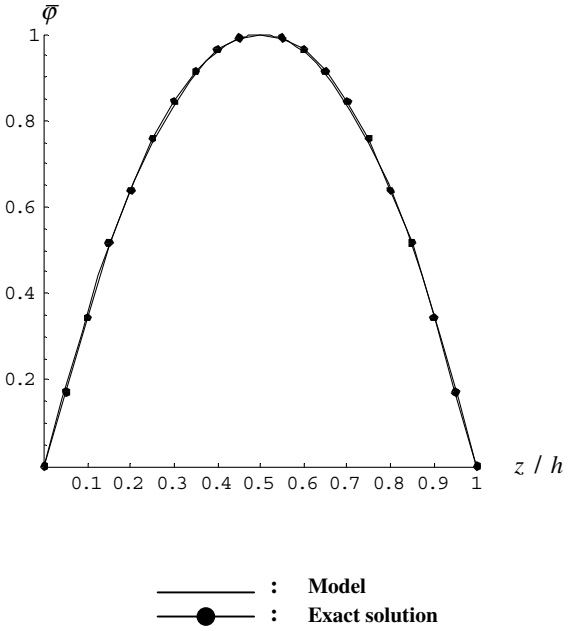

Fig. 6. Thickness distribution of the normalized electrostatic potential $\bar{\varphi}$, single-layered shell, $R = 100$ h.

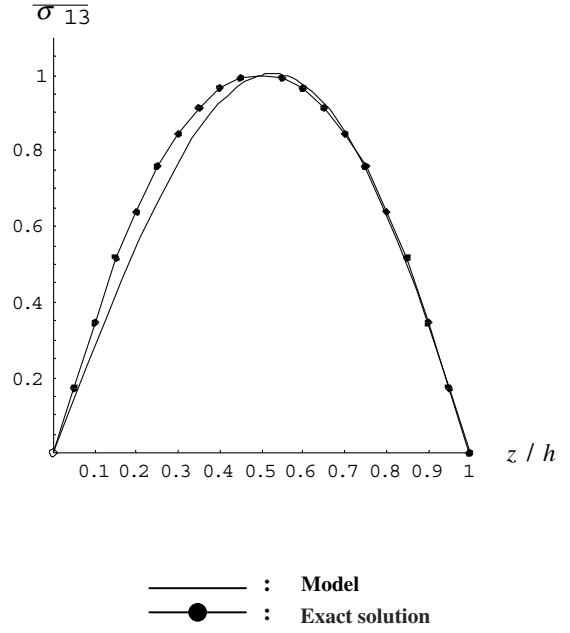

Fig. 7. Thickness distribution of the normalized shear-stress $\bar{\sigma}_{13}$, single-layered shell, $R = 4$ h.

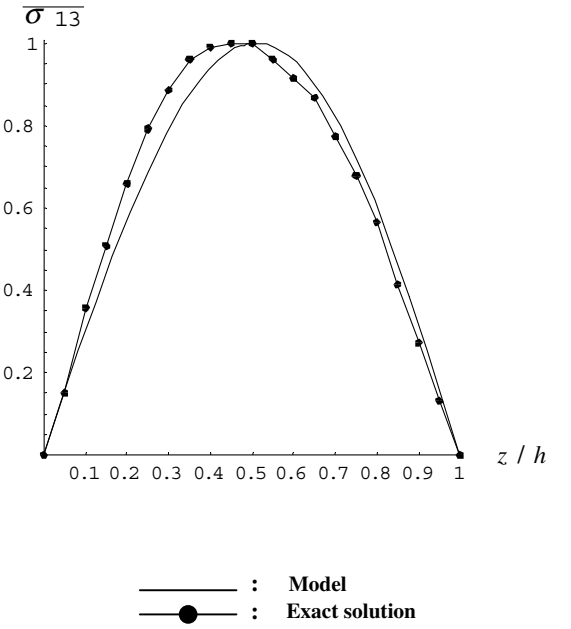

Fig. 8. Thickness distribution of the normalized shear-stress $\bar{\sigma}_{13}$, single-layered shell, $R = 10$ h.

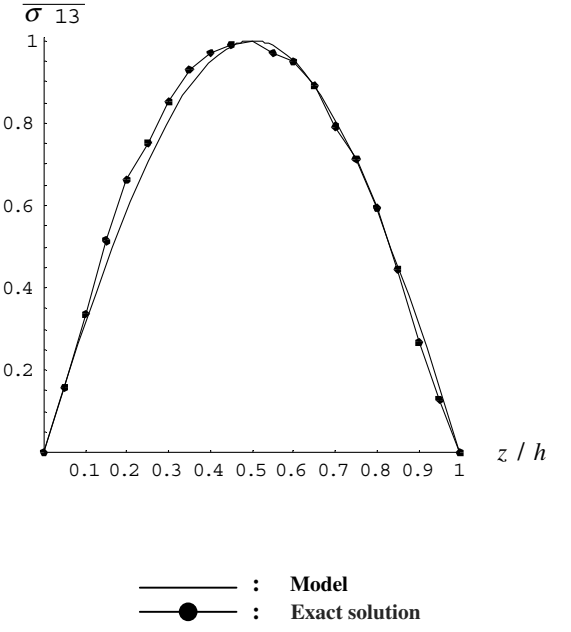

Fig. 9. Thickness distribution of the normalized shear-stress $\bar{\sigma}_{13}$, single-layered shell, $R = 100$ h.

It can be noted that our model yields very accurate results as concerns the electrostatic potential, as it can be seen in Figs. 4–6. As for the transverse shear-stress, the expected gap due to the effects of curvature can be observed, in Figs. 7–9. The results become closer of the three-dimensional solution as the shell grows thinner, as it could be expected.

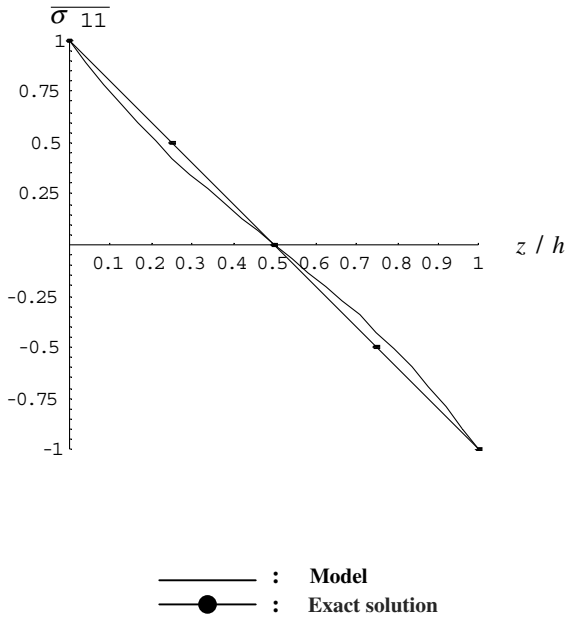

Fig. 10. Thickness distribution of the normalized in-plane-stress $\bar{\sigma}_{11}$, single-layered shell, $R = 4$ h.

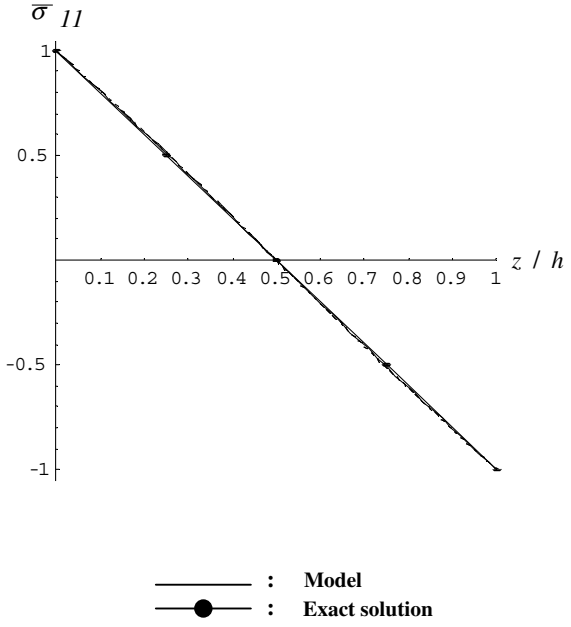

Fig. 11. Thickness distribution of the normalized in-plane-stress $\bar{\sigma}_{11}$, single-layered shell, $R = 10$ h.

4. Application of the piezoelectric shell model

We present here another application of our piezoelectric shell model. For the case we present, there is not any exact solution. Results we obtain appear in fact as extensions of results obtained for similar cases with plates [34].

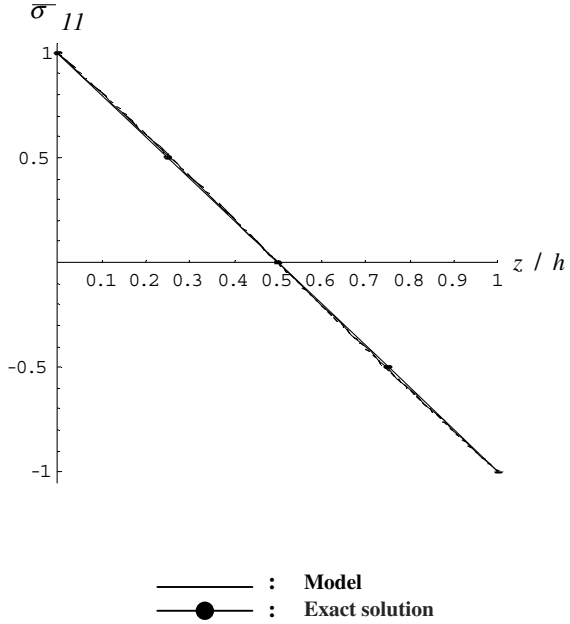

Fig. 12. Thickness distribution of the normalized in-plane-stress $\bar{\sigma}_{11}$, single-layered shell, $R = 100$ h.

For this example, we consider infinitely long, simply supported, two-layered, orthotropic, piezoelectric, radially polarized, circular cylindrical shell panels in cylindrical bending, under pressure and electrostatic excitation. We denote by R their mean radius, by h their thickness, and α their angular span (see Fig. 3).

Their lateral surfaces are subjected to electrical and traction boundary conditions independent of the thickness coordinate.

The stresses, strains, displacements, electric field and potential do not depend on the x_2 variable. The displacement U_2 playing no role, it can be cancelled out.

The height of the panels is fixed at $h = 0.01$ m and their angular span to $\alpha = \pi/3$.

The simple support conditions for the panel are simulated as in Eq. (66).

We consider here a piezoelectric bimorph shell, made of PZT4 material (see properties Table 1). The shell is supposed to be simply supported, and subject to an applied electrostatic potential on the top $(+V)$ and bottom faces $(-V)$ (see Fig. 13):

$$V(x_1) = V_0 \sin p_1 x_1, \tag{81}$$

where

$$p_1 = \pi/\alpha. \tag{82}$$

The shear stresses on the top and bottom faces are specified to be zero.

The approximation of the electrostatic potential is given by Eqs. (22)–(25).

The prescribed conditions on the electrostatic potential are

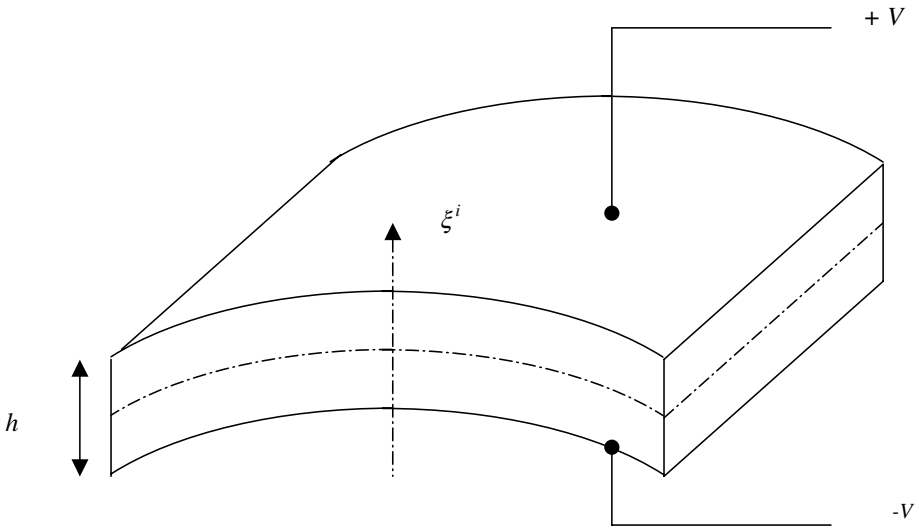

Fig. 13. The bimorph shell, with imposed potentials.

$$\varphi^{1B}(x_\alpha) = -V, \quad \varphi^{3B}(x_\alpha) = V. \tag{83}$$

Moreover, the symmetry allows to write

$$\varphi^{2B}(x_\alpha) = 0, \quad \varphi^{2M}(x_\alpha) = -\varphi^{1M}(x_\alpha). \tag{84}$$

Thus, the potential is given by

$$\varphi(x_j) = \left[-\frac{1}{2}\xi^1(\xi^1 - 1)V + (1 - (\xi^1)^2)\varphi^{1M}(x_\alpha) \right]\chi^1 + \left[-(1 - (\xi^2)^2)\varphi^{1M}(x_\alpha) + \frac{1}{2}\xi^2(\xi^2 + 1)V \right]\chi^2. \tag{85}$$

The dielectric coefficients of the two layers being identical, no continuity of the uncoupled electrical displacement needs to be taken into account.

As for the preceding problem, the mechanical generalized displacements remaining unknowns are u_1, w, γ_1^0.

From Eq. (85), it is evident that the electrical generalized unknown is φ^{1M}.

The solution of the corresponding boundary-value problem, in terms of the generalized unkowns given by Eq. (52), is searched under the same form as the one stated in Eqs. (74) and (75).

Substituting these expressions into the equilibrium equations given by Eqs. (40)–(46), with Eqs. (20), (37) and (85), a linear system of the following form is obtained:

$$K^2 X = B^{2'}, \tag{86}$$

where

$$X^2 = (A_1, B, C_1, \Phi_1). \tag{87}$$

The coefficients of K^2 and $B^{2'}$ are given in Appendix B.

With Eqs. (20), (36) and (37), the displacement, strain and stress components, and the electrostatic potential can be calculated.

The through the thickness distribution of the normalized electrostatic potential

$$\bar{\varphi}(z) = \frac{\bar{\varphi}\left(\theta = \frac{\alpha}{2}, z\right)}{\varphi\left(\theta = \frac{\alpha}{2}, h\right)}, \tag{88}$$

the normalized longitudinal displacement at $x_1 = 0$,

$$\bar{U}_1(z) = \frac{U_1(\theta = 0, z)}{U_1(\theta = 0, 0)}, \tag{89}$$

the normalized transverse shear-stress

$$\bar{\sigma}_{13}(z) = \frac{\sigma_{13}(\theta = 0, z)}{\sigma_{13}\left(\theta = 0, \frac{h}{2}\right)}, \tag{90}$$

and the normalized in plane stress

$$\bar{\sigma}_{11}(z) = \frac{\sigma_{11}\left(\theta = \frac{\alpha}{2}, z\right)}{\sigma_{11}^{(1)}\left(\theta = \frac{\alpha}{2}, 0\right)} \tag{91}$$

are shown in Figs. 14–17, $\sigma_{11}^{(1)}$ being the in plane stress calculated in the first layer.

Results obtained for this case represents an extension of similar results obtained in the case of plates [34]. As expected, the general aspect of the curves is the same, with of course the effect of the curvature. The adequation to those results, added to the fact that we have

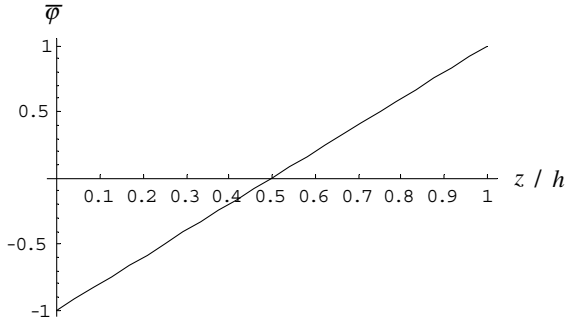

Fig. 14. Thickness distribution of the normalized electrostatic potential $\bar{\varphi}$, bimorph shell, $R = 4$ h.

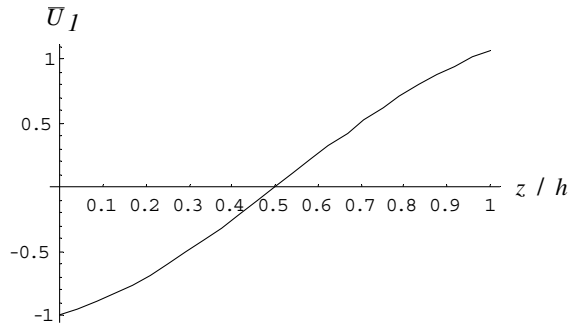

Fig. 15. Thickness distribution of the normalized in-plane displacement $\bar{U}_1$, bimorph shell, $R = 4$ h.

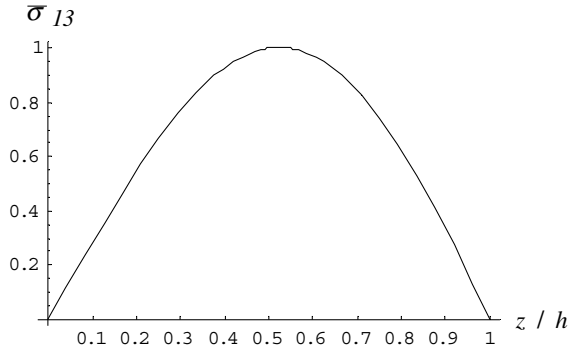

Fig. 16. Thickness distribution of the normalized shear-stress $\bar{\sigma}_{13}$, bimorph shell, $R = 4$ h.

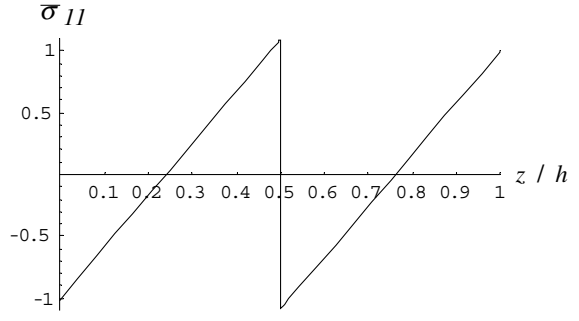

Fig. 17. Thickness distribution of the normalized in-plane stress $\bar{\sigma}_{11}$, bimorph.

presented tough cases, i.e., deep shells ($R = 4h$), show that our model can be used to study piezoelectric structures submitted to different kinds of electromechanical loadings.

5. Conclusion

In this paper, a new refined two-dimensional piezoelectric shell theory, which allows to satisfy the compatibility conditions for displacements and the electrostatic potential at layer interfaces, as well as the boundary conditions, is proposed. This theory also takes into account refinements of the shear and membrane terms, by means of trigonometric functions. The accuracy of the model is assessed by applying the theory to problems for which exists a three-dimensional solution: first, a multilayered plate, second, a single-layered shell. Applications are then proposed: bimorph shells with imposed electrostatic potentials. It appears that the present model is of simple use, incorporating only five independent generalized displacements and one or two independent generalized electrostatic potentials as unknowns. This is obtained from the exact "satisfaction" of boundary and interface conditions independently for mechanics and electricity (potential and electric displacement), which is the first time within a layer-wise approach. It results in reducing the number of unknowns. Then, the coupled piezoelectric model is deduced from the boundary-value problem, where we use the coupled piezoelectric law for the above mechanical and electric fields satisfying separately all the boundary conditions. This is the novelty of our approach linked to a refined multilayered shell theory. Results show that this approach is numerically consistent with prescribed interface and boundary conditions. Eventually, they are in very good agreement with the exact three-dimensional solution. It is important to note that our model is probably the one that incorporates the fewest unknowns (independent generalized displacements and electrostatic potentials).

Appendix A

The stiffness matrix K^1 used for example 3.1 is given by

$$K^1 = \begin{bmatrix} K^1_{11} & K^1_{12} & K^1_{13} & K^1_{14} & K^1_{15} & K^1_{16} & K^1_{17} \\ & K^1_{22} & K^1_{23} & K^1_{24} & K^1_{25} & K^1_{26} & K^1_{27} \\ & & K^1_{33} & K^1_{34} & K^1_{35} & K^1_{36} & K^1_{37} \\ & & & K^1_{44} & K^1_{45} & K^1_{46} & K^1_{47} \\ & & & & K^1_{55} & K^1_{56} & K^1_{57} \\ & & \text{SYM} & & & K^1_{66} & K^1_{67} \\ & & & & & & K^1_{77} \end{bmatrix},$$

where

$$K^1_{11} = \int_0^h \left\{ p^2 C^*_{11} + \frac{1}{2} q^2 C^*_{66} \right\} \mathrm{d}z,$$

$$K^1_{12} = \int_0^h \left\{ pq C^*_{12} + \frac{1}{2} pq C^*_{66} \right\} \mathrm{d}z,$$

$$K^1_{13} = \int_0^h \left\{ -p\left[p^2 C^*_{11} + q^2 C^*_{12}\right] - pq^2 C^*_{66} \right\} z \, \mathrm{d}z,$$

$$K^1_{14} = \int_0^h \{p^2 C^*_{11} + q^2 C^*_{66}\} h_1(z)\,\mathrm{d}z,$$

$$K^1_{15} = \int_0^h \{pq C^*_{12} + pq C^*_{66}\} h_2(z)\,\mathrm{d}z,$$

$$K^1_{16} = -\int_0^h p e^*_{31} Q^{1\mathrm{M}'}(z)\,\mathrm{d}z,$$

$$K^1_{17} = -\int_0^h p e^*_{31} Q^{2\mathrm{M}'}(z)\,\mathrm{d}z,$$

$$K^1_{22} = \int_0^h \{q^2 C^*_{22} + p^2 C^*_{66}\}\,\mathrm{d}z,$$

$$K^1_{23} = \int_0^h \{ -q[p^2 C^*_{12} + q^2 C^*_{22}] - qp^2 C^*_{66}\} z\,\mathrm{d}z,$$

$$K^1_{24} = \int_0^h \{pq C^*_{12} + pq C^*_{66}\} h_1(z)\,\mathrm{d}z,$$

$$K^1_{25} = \int_0^h \{q^2 C^*_{22} + p^2 C^*_{66}\} h_2(z)\,\mathrm{d}z,$$

$$K^1_{26} = -\int_0^h q e^*_{32} Q^{1\mathrm{M}'}(z)\,\mathrm{d}z,$$

$$K^1_{27} = -\int_0^h q e^*_{32} Q^{2\mathrm{M}'}(z)\,\mathrm{d}z,$$

$$K^1_{34} = \int_0^h \{ -p^3 C^*_{11} - pq^2 C^*_{12} - pq^2 C^*_{66}\} z h_1(z)\,\mathrm{d}z,$$

$$K^1_{35} = \int_0^h \{ -q^3 C^*_{12} - p^2 q C^*_{22} - p^2 q C^*_{66}\} z h_2(z)\,\mathrm{d}z,$$

$$K^1_{36} = \int_0^h \{p^2 e^*_{31} + q^2 e^*_{32}\} Q^{1\mathrm{M}'}(z)\,\mathrm{d}z,$$

$$K^1_{37} = \int_0^h \{p^2 e^*_{31} + q^2 e^*_{32}\} Q^{2\mathrm{M}'}(z)\,\mathrm{d}z,$$

$$K^1_{44} = \int_0^h \left\{ [p^2 C^*_{11} + pq C^*_{66}] h_1^2(z) + \frac{1}{2} C^*_{55} h_1'^2(z) \right\} \mathrm{d}z,$$

$$K^1_{45} = \int_0^h \{pq C^*_{12} + pq C^*_{66}\} h_1(z) h_2(z)\,\mathrm{d}z,$$

$$K^1_{46} = -\int_0^h p e^*_{31} Q^{1\mathrm{M}'}(z) h_1(z)\,\mathrm{d}z,$$

$$K^1_{47} = -\int_0^h p e^*_{31} Q^{2\mathrm{M}'}(z) h_1(z)\,\mathrm{d}z,$$

$$K^1_{55} = \int_0^h \left\{ \left[q^2 C^*_{22} + \frac{1}{2} pq C^*_{66} \right] h_2^2(z) + C^*_{44} h_2'^2(z) \right\} \mathrm{d}z,$$

$$K^1_{56} = -\int_0^h q e^*_{32} Q^{1\mathrm{M}'}(z) h_2(z)\,\mathrm{d}z,$$

$$K^1_{57} = -\int_0^h q e^*_{32} Q^{2\mathrm{M}'}(z) h_2(z)\,\mathrm{d}z,$$

$$K^1_{66} = -\int_0^h \left\{ [p^2 \varepsilon^*_{11} + q^2 \varepsilon^*_{22}] Q^{1\mathrm{M}^2}(z) + \varepsilon^*_{33} Q^{1\mathrm{M}'^2}(z) \right\} \mathrm{d}z,$$

$$K^1_{67} = -\int_0^h \left\{ [p^2 \varepsilon^*_{11} + q^2 \varepsilon^*_{22}] Q^{1\mathrm{M}}(z) Q^{2\mathrm{M}}(z) + \varepsilon^*_{33} Q^{1\mathrm{M}'}(z) Q^{2\mathrm{M}'}(z) \right\} \mathrm{d}z,$$

$$K^1_{77} = -\int_0^h \left\{ [p^2 \varepsilon^*_{11} + q^2 \varepsilon^*_{22}] Q^{2\mathrm{M}^2}(z) + \varepsilon^*_{33} Q^{2\mathrm{M}'^2}(z) \right\} \mathrm{d}z,$$

where $Q^{1\mathrm{M}}, Q^{2\mathrm{M}}$, are given in Section 3, coefficients K^1_{IJ} of this matrix being computed by the numerical integration of Gauss.

The mass matrix M used in example 3.1 is given by

$$M = \begin{bmatrix} I_1 & 0 & -pI_2 & I_3^{(1)} & 0 & 0 & 0 \\ & I_1 & -qI_2 & 0 & I_3^{(2)} & 0 & 0 \\ & & I_1 + (p^2+q^2)I_4 & -pI_5^{(1)} & -qI_5^{(2)} & 0 & 0 \\ & & & I_6^{(1)} & & 0 & 0 \\ & & & & I_6^{(2)} & 0 & 0 \\ & & \mathrm{SYM} & & & 0 & 0 \\ & & & & & 0 & 0 \end{bmatrix}.$$

Inertia coefficients in M, calculated from Eq. (45), are integrated numerically using the Gauss rule.

Appendix B

The stiffness matrix K^2 used for the example 3.1 is given by:

$$K^2 = \begin{bmatrix} K^2_{11} & K^2_{12} & K^2_{13} & K^2_{14} \\ & K^2_{22} & K^2_{23} & K^2_{24} \\ & & K^2_{33} & K^2_{34} \\ & \mathrm{SYM} & & K^2_{44} \end{bmatrix},$$

where

$$K^2_{11} = \int_0^h p_1^2 C^*_{11} \mu^5\,\mathrm{d}z,$$

$$K^2_{12} = \int_0^h \{ -p_1^3 C^*_{11} z \mu^4 + p_1^2 C^*_{11} b_{11} \mu^4\}\,\mathrm{d}z,$$

$$K^2_{13} = \int_0^h p_1^2 C^*_{11} h_1(z) \mu^4\,\mathrm{d}z,$$

$$K^2_{14} = -\int_0^h p_1 e^*_{31} Q^{1\mathrm{M}'}(z) \mu^3\,\mathrm{d}z,$$

$$K_{22}^2 = \int_0^h \left\{ p_1^4 C_{11}^* z^2 \mu^3 - p_1^3 C_{11}^* b_{11} z \mu^3 + p_1 C_{11}^* b_{11}^2 \mu^3 \right\} \mathrm{d}z,$$

$$K_{23}^2 = \int_0^h \left\{ - p_1^3 C_{11}^* z h_1(z) \mu^3 + p_1 C_{11}^* h_1(z) b_{11} \mu^3 \right\} \mathrm{d}z,$$

$$K_{24}^2 = \int_0^h \left\{ p_1^2 e_{31}^* Q^{1M'}(z) z \mu^2 - p_1 e_{31}^* Q^{1M'}(z) b_{11} \mu^2 \right\} \mathrm{d}z,$$

$$K_{33}^2 = \int_0^h \left\{ p_1^2 C_{11}^* h_1^2(z) \mu^3 + C_{55}^* \left[\mu h_1'(z) + b_1^1 h_1(z) \right]^2 \mu \right\} \mathrm{d}z,$$

$$K_{34}^2 = \int_0^h \left\{ - p_1 e_{31}^* Q^{1M'}(z) h_1(z) \mu^2 + p_1 e_{24}^* \frac{Q^{1M}(z)}{R+z} h_1(z) \left[\mu h_1'(z) + b_1^1 h_1(z) \right] \mu \right\} \mathrm{d}z,$$

$$K_{44}^2 = - \int_0^h \left\{ p_1^2 \frac{\varepsilon_{11}^*}{R+z} Q^{1M^2}(z) + \varepsilon_{33}^* Q^{1M'^2}(z) \right\} \mu \, \mathrm{d}z$$

and

$$B^{2\prime} = \begin{bmatrix} B_1 \\ B_2 - p_0 \mu_h \\ B_3 \\ B_4 \end{bmatrix},$$

$$B_1 = \int_0^h p_1 e_{31}^* Q_V'(z) \bar{V}_0 \mu^3 \, \mathrm{d}z,$$

$$B_2 = - \int_0^h \left\{ p_1^2 e_{31}^* Q_V'(z) \bar{V}_0 z \mu^2 - p_1 e_{31}^* Q_V'(z) \bar{V}_0 b_{11} \mu^2 \right\} \mathrm{d}z,$$

$$B_3 = - \int_0^h \left\{ - p_1 e_{31}^* Q_V'(z) \bar{V}_0 h_1(z) \mu^2 + p_1 e_{24}^* \frac{Q_V'(z) \bar{V}_0}{R+z} h_1(z) \left[\mu h_1'(z) + b_1^1 h_1(z) \right] \mu \right\} \mathrm{d}z,$$

$$B_4 = \int_0^h \left\{ p_1^2 \frac{\varepsilon_{11}^*}{R+z} Q^{1M}(z) Q^V(z) \bar{V}_0 + \varepsilon_{33}^* Q^{1M}(z) Q_V'(z) \bar{V}_0 \right\} \mu \, \mathrm{d}z,$$

where $\bar{V}_0 = \frac{C_0 V_0}{E_0}$.

References

[1] Toupin RA. Piezoelectric relations and the radial deformation of polarized spherical shells. J Acoust Soc Am 1959;31:315–518.

[2] Adelman NT, Stavsky Y. Axisymmetric vibrations of radially polarized piezoelectric ceramic cylindres. J Acoust Soc Am 1975;38:245–54.

[3] Adelman NT, Stavsky Y. Axisymmetric vibrations of radially polarized composite cylinders and discs. J Acoust Soc Am 1975;43:37–44.

[4] Sun CT, Cheng NC. Piezoelectric waves on a layered cylinder. J Appl Phys 1974;45:4288–92.

[5] Karlash VL. Dynamic stresses in a compound piezoceramic hollow cylinder. Prikl Mekh 1987;23:49–54.

[6] Paul HS, Nelson VK, Vazhapadi K. Flexural vibrations of piezoelectric composite cylinder. J Acoust Soc Am 1996;99(1):309–13.

[7] Paul HS, Vankatesan M. Axisymmetric vibration of a piezoelectric solid cylinder guided by a thin film. J Acoust Soc Am 1986;80:1091–6.

[8] Siao JCT, Dong SB, Song J. Frequency spectra of laminated piezoelectric cylinders. J Vib Acoust 1994;116(3):364–70.

[9] Mitchell JA, Reddy JNA. study of embedded piezoelectric layers in composite cylinders. J Appl Mech 1995;62(1):166–73.

[10] Xu KM, Noor AK. 3-Dimensional analytical solutions for coupled thermoelectroelastic response of multilayered cylindrical shells. AAIA J 1996;34(4):110–5.

[11] Heyliger PR. A note on the static behavior of simply supported laminated piezoelectric cylinders. Int J Solids Struct 1997;34(29):3781–94.

[12] Dumir PC, Dube GP, Kapuria S. Exact piezoelastic solution of simply supported orthotropic circular cylindrical panel in cylindrical bending. Int J Solids Struct 1997;34(6):685–702.

[13] Drumheller DS, Kalnins A. Dynamic shell theory for ferroelectric ceramics. J Acoust Soc Am 1970;47:1343–8.

[14] Haskins DS, Kalnins A. Dynamic shell theory for ferroelectric ceramics. J Acoust Soc Am 1970;47:1343–8.

[15] Tzou HS, Garde M. Theoretical analysis of a multilayered thin shell coupled with piezoelectric shell actuators for distributed vibration controls. J Sound Vib 1989;132(3):433–50.

[16] Tzou HS, Zhong JP. Electromechanics and vibrations of piezoelectric shell distributed systems. J Dyn Syst Measure Contr 1993;115(3):506–17.

[17] Tzou HS. Piezoelectric shells: distributed sensing and control of continua. Norwell, MA: Kluwer Academic Publishers; 1993.

[18] Lammering R. The application of a shell finite element for composites containing piezoelectric polymers in vibration control. Comput Struct 1995;41(5):1101–9.

[19] Koconis DB, Kollar LP, Springer GS. Shape control of composite plates and shells with embedded actuators. I. Voltages specified. J Compos Mater 1994;28(5):415–58.

[20] Tzou HS, Ye R. Analysis of piezoelastic structures with laminated piezoelectric triangle shell elements. AIAA J 1996;34(1):110–5.

[21] Heyliger PR, Pei KC, Saravanos DA. Layerwise mechanics and finite element model for laminated piezoelectric shell. AIAA J 1996;34(11):2353–60.

[22] Saravanos DA. Coupled mixed-field laminate theory and finite element for smart piezoelectric shell structures. AIAA J 1997;35(8):1327–33.

[23] Ossadzow C, Muller P, Touratier M. Wave dispersion in deep multilayered doubly curved viscoelastic shells. J Sound Vib 1998;214(3):531–52.

[24] Ossadzow C, Touratier M, Muller P. A deep doubly curved multilayered shell theory. AIAA J 1999;37(1):100–9.

[25] Naghdi PM. The theory of shells and plates. In: S. Flügge, editor. Handbuch der Physik, vol. VIa/2. Berlin: Springer; 1972. p. 425–640.

[26] Touratier M. A refined theory of laminated shallow shells. Int J Solids Struct 1992;29(11):1401–15.

[27] Di Sciuva M. An improved third-order shear deformation theory for moderately thick multilayered anisotropic shells and plates. J Appl Mech 1987;54:589–96.

[28] He L-H. A linear theory of laminated shells accounting for continuity of displacements and transverse shear stresses at layer interfaces. Int J Solids Struct 1994;31(5):613–27.

[29] Cheng S. Elasticity theory of plates and a refined theory. J Appl Mech 1979;46(3):644–50.

[30] Touratier M. A refined theory for thick composite plates. Mech Res Commun 1988;15(4):229–36.

[31] Tiersten HF. Linear piezoelectric plate vibrations. New York: Plenum; 1969.
[32] Heyliger P. Exact free-vibration analysis of laminated plates with embedded piezoelectric layers. J Acoust Soc Am 1995;98(3): 1547–57.
[33] Wolfram S. The mathematica book. 4th ed. Mathematica version 4. AAA: Cambridge University Press; 1999.
[34] Fernandes A. Modeling and study of piezoelectric components: applications to multifunctional structures. Ph.D. thesis, Université Paris VI; 2000 [in French].